

## Quantitative determination of electric and magnetic second-order susceptibility tensors of chiral surfaces

Martti Kauranen, Jeffery J. Maki, Thierry Verbiest, Sven Van Elshocht, and André Persoons

Laboratory of Chemical and Biological Dynamics and Center for Research on Molecular Electronics and Photonics,  
University of Leuven, B-3001 Heverlee, Belgium

(Received 19 September 1996)

We present a measurement technique to determine the relative values of all components of the three tensors that describe second-harmonic generation from chiral isotropic surfaces up to first order in the magnetic-dipole interaction. For a thin film of a chiral polymer, the largest tensor components involving magnetic interactions are nonvanishing only because of chirality and their magnitudes are  $\sim 20\%$  of the largest electric-dipole-only components. These chiral magnetic components are larger than the chiral electric component. [S0163-1829(97)51904-7]

Chiral molecules occur in two enantiomers that are mirror images of each other. Such molecules are optically active, i.e., they interact differently with left- and right-hand circularly polarized light.<sup>1</sup> Optical activity arises from contributions of magnetic-dipole transitions to the linear optical properties of chiral materials. Nonlinear optical properties of chiral materials have been investigated both theoretically<sup>2</sup> and experimentally.<sup>3-9</sup> Second-harmonic generation from isotropic chiral surfaces and thin films has been found to respond differently to the two opposite circular polarizations of fundamental light.<sup>5-7</sup> Such nonlinear optical activity has been analyzed within the electric-dipole approximation,<sup>10,11</sup> and with the inclusion of the magnetic contributions to the nonlinearity.<sup>6,7,12-14</sup> The largest second-order susceptibility components involving magnetic transitions were estimated to be  $\sim 10\%$  of the electric-dipole-only components.<sup>7,14</sup> However, these early reports used a simplified phenomenological model to analyze the experimental data. Hence there is continued need to address the relative strengths of electric and magnetic contributions to the nonlinear response of chiral materials in a more quantitative way.

In this paper, we present a quantitative characterization of the second-order nonlinear response of a chiral surface. The surface we use consists of a thin film of a chiral polymer. We use a recently proposed technique<sup>14,15</sup> to determine the relative values of all components of the tensors that describe second-harmonic generation from chiral surfaces up to first order in the magnetic-dipole interaction.<sup>16</sup> The intensities of several second-harmonic signals are measured as functions of the state of polarization of the fundamental field. Only normalized line shapes of  $p$ - and  $s$ -polarized signals need to be measured. This is a distinct advantage compared to similar measurements on achiral surfaces, which require mutually calibrated signals or mixing of  $p$ - and  $s$ -polarized signals.<sup>17</sup>

For a theoretical description, the nonlinear polarization is taken to be<sup>13</sup>

$$P_i(2\omega) = \sum_{j,k} [\chi_{ijk}^{eee} E_j(\omega) E_k(\omega) + \chi_{ijk}^{eem} E_j(\omega) B_k(\omega)],$$

where  $\mathbf{E}(\omega)$  and  $\mathbf{B}(\omega)$  are the electric field and magnetic-induction field at the fundamental frequency. In addition, the

medium develops a nonlinear magnetization

$$M_i(2\omega) = \sum_{j,k} \chi_{ijk}^{mee} E_j(\omega) E_k(\omega),$$

The independent nonvanishing components of the tensors  $\chi^{eee}$ ,  $\chi^{eem}$ , and  $\chi^{mee}$  for isotropic surfaces and thin films ( $C_\infty$  symmetry) (Refs. 7 and 13) are given in Table I. Some components are allowed for all isotropic surfaces (achiral components), whereas the remaining components are allowed only for chiral surfaces (chiral components).

The intensity of any component of the second-harmonic field can be expanded as<sup>13</sup>

$$I(2\omega) = |fE_p^2(\omega) + gE_s^2(\omega) + hE_s(\omega)E_p(\omega)|^2, \quad (1)$$

TABLE I. Independent components of tensors  $\chi^{eee}$ ,  $\chi^{eem}$ , and  $\chi^{mee}$  in the geometry of Fig. 1. Boldface indicates a chiral component. The determined values are normalized to  $\chi_{xxz}^{eee} = 1$ . The numbers in parentheses are estimated errors in each value. The magnitudes are normalized to that of  $\chi_{zzz}^{eee}$ . The tensor components essential to our model are indicated by an asterisk.

Tensor	Component	Determined value	Magnitude
$\chi^{eee}$	$zzz$ (*)	1.571(0.829) - $i$ 0.583(0.567)	100%
	$xxz$ (*)	1.00	60%
	$zxx$ (*)	1.034(0.085) - $i$ 0.136(0.075)	62%
	<b><math>xyz</math></b> (*)	0.110(0.006) + $i$ 0.065(0.004)	7.6%
$\chi^{eem}$	<b><math>zzz</math></b> (*)	0.354(0.157) - $i$ 0.152(0.134)	23%
	<b><math>zxx</math></b> (*)	0.194(0.094) - $i$ 0.068(0.083)	12%
	<b><math>zxz</math></b> (*)	0.049(0.030) - $i$ 0.069(0.029)	5.1%
	<b><math>xxz</math></b>	-0.011(0.019) + $i$ 0.014(0.020)	1.1%
	$xyz$ (*)	0.019(0.038) - $i$ 0.102(0.064)	6.2%
	$xzy$	-0.015(0.137) + $i$ 0.223(0.201)	13%
	$zxy$	0.051(0.146) + $i$ 0.083(0.154)	5.8%
$\chi^{mee}$	<b><math>zzz</math></b> (*)	0.163(0.143) - $i$ 0.195(0.135)	15%
	<b><math>zxx</math></b>	-0.001(0.014) - $i$ 0.004(0.020)	0.3%
	<b><math>xxz</math></b>	0.005(0.007) - $i$ 0.005(0.006)	0.4%
	$xyz$	0.027(0.034) - $i$ 0.035(0.047)	2.6%

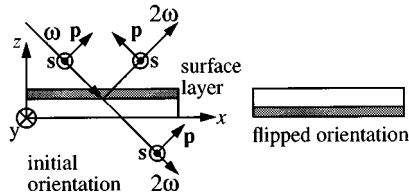


FIG. 1. Geometry of second-harmonic generation from a chiral surface. The two orientations of the sample are related by the coordinate transformation  $x \rightarrow x$ ,  $y \rightarrow -y$ , and  $z \rightarrow -z$ .

where  $E_p(\omega)$  and  $E_s(\omega)$  are the  $p$ - and  $s$ -polarized components of the fundamental field (Fig. 1). The coefficients  $f$ ,  $g$ , and  $h$  are unique to each second-harmonic signal, and depend on the three susceptibility tensors and on the Fresnel factors at the fundamental and second-harmonic frequencies.<sup>13</sup> For the present work, we have generalized the results of Ref. 13 to also include in these coefficients the effects of propagation in a thin film of finite thickness.<sup>18</sup> In our experiments, a quarter-wave plate is used to continuously vary the relative phase and amplitude of the fundamental field components.<sup>15</sup> The measured second-harmonic line shapes are fitted to the functional form of Eq. (1) to determine the values of  $f$ ,  $g$ , and  $h$ . This fit is unique within an overall phase factor.<sup>15</sup> Only relative values of the coefficients need to be known,<sup>15</sup> and so we normalize  $h=1$  for each line shape.

We normalize the relative values of the tensor components to  $\chi_{xxz}^{eee}=1$ . The task is then to determine the complex values of the other 14 tensor components. A sufficient number of eight independent measurements is provided by the  $p$ - and  $s$ -polarized components of the reflected and transmitted second-harmonic signals for the two orientations of the sample shown in Fig. 1. The change in the sample orientation corresponds to a coordinate transformation that reverses the sign of certain tensor components. The sign reversals, together with changes in the Fresnel factors, provide strong decoupling of the various tensor components within each expansion coefficient. The eight fitted line shapes are made mutually compatible by scaling each of them by a complex factor to yield 24 complex equations of the type

$$f_i^{\text{theoretical}}(\chi^{eee}, \chi^{eem}, \chi^{mee}) = c_i f_i^{\text{fitted}},$$

where  $f_i^{\text{theoretical}}$  depends linearly on the components of the three tensors,  $c_i$  is a complex scaling factor unique to each measured signal, and  $f_i^{\text{fitted}}$  is the value of coefficient  $f$  for signal  $i$  relative to  $h_i^{\text{fitted}}=1$ . The eight scaling factors  $c_i$  are additional unknown quantities, which are solved for together with the unknown tensor components to obtain a self-consistent solution to the set of equations. The procedure thus has 22 unknowns and 24 equations.

In our experiments, the fundamental beam of a  $Q$ -switched and injection-seeded Nd:YAG (yttrium aluminum garnet) laser (1064 nm, 50 Hz,  $\sim 10$  ns,  $\sim 10$  mJ) was applied at a  $45^\circ$  angle of incidence with respect to the sample. The experimental setup was similar to that of Ref. 14, but with improved optical components. Extreme care was taken in the proper alignment of the setup and in verifying its polarization purity. The laser beam had a diameter of  $\sim 1$  mm at the sample to facilitate alignment to the same spot for

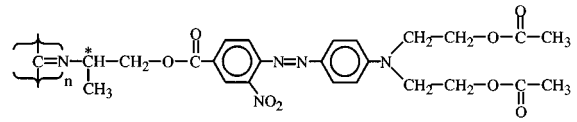


FIG. 2. Structure of the chiral nonlinear poly(isocyanide).

the two orientations. The chiral sample was a Langmuir-Blodgett film of an  $S$  enantiomer of a nonlinear poly(isocyanide) (Fig. 2) (Ref. 19) mixed with poly( $S$ -1-acetoxymethylethylisocyanide). The 18-layer sample with a total thickness of  $\sim 35$  nm was deposited on a glass substrate. Several tests were performed to verify the in-plane isotropy of the sample. Vanishing of the second-harmonic signal at normal incidence rules out any anisotropic symmetry except  $C_2$ . This group was excluded by rotating the sample about the surface normal at  $45^\circ$  angle of incidence. No evidence of the birefringence of the substrate was observed. The absorbance of the sample at the second-harmonic wavelength 532 nm was  $\sim 50\%$  of the maximum absorbance ( $\sim 0.065$  at 457 nm). To account for the Fresnel factors, the refractive indices of the film at the fundamental and second-harmonic wavelengths were 1.53 and  $1.90 + i0.10$ , respectively. The indices of the substrate at these wavelengths were 1.51 and 1.52, respectively.

Each measurement was repeated three times. Our experimental results (Fig. 3) are very clean, which allows the determination of most coefficients  $f$ ,  $g$ , and  $h$  to better than 2% (and often better than 1%) accuracy. However, the  $g$  coefficients of the  $s$ -polarized signals are small ( $\sim 0.01$  relative to  $h$ ) and their accuracy poor ( $\sim 20$ – $30\%$ ). These coefficients can only be nonvanishing because of magnetic contributions to the nonlinearity. We have verified by simulations that, in the limit where these coefficients vanish, their fitted values could be due to the residual noise in our data or small ( $\sim \lambda/250$ ) waveplate retardation errors. Hence we have first attempted to explain our results in the electric-dipole approximation. However, the four independent solutions<sup>15</sup> to the components of  $\chi^{eee}$  (Table II) are mutually incompatible, and we conclude that our results cannot be explained in the electric-dipole approximation.

We next include the magnetic contributions to the nonlinearity. The inaccuracy of the  $g$  coefficients of the  $s$ -polarized signals is not detrimental to our technique, since we avoid the quantitative use of this information. As a consequence, however, the number of equations in the model is reduced to 20, although 22 unknown quantities remain. We proceed by assuming that any two magnetic tensor components vanish, and solving for the remaining 20 unknowns. The  $g$  coefficients of the  $s$ -polarized signals are then calculated for each solution to assess its quality. Any solution that leads to excessively large values of these coefficients is rejected. Acceptable solutions are found only when the vanishing tensor components belong to a subset of all magnetic components. These solutions are very stable, independent of which two components are assumed to vanish and of the exact value of the rejection threshold. This is of course due to the fact that several magnetic components are small. The final solution to the set of equations (Table I) is obtained as an average of the acceptable solutions.

Since our procedure is based on solving a large number

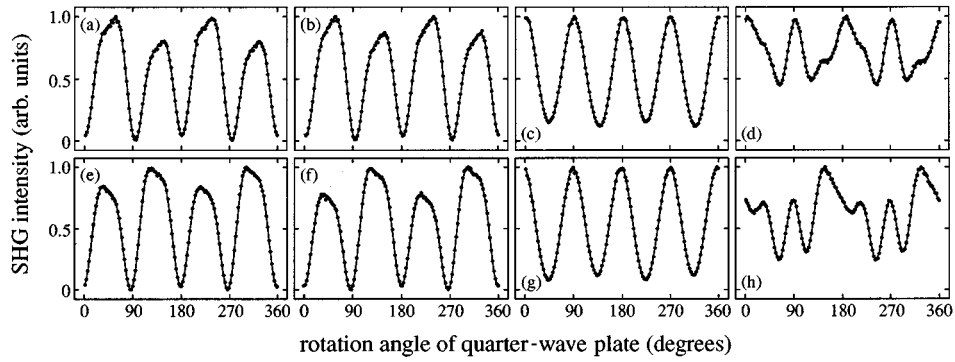


FIG. 3. The eight measured second-harmonic signals. The wave plate rotation angle of  $0^\circ$  corresponds to  $p$ -polarized fundamental field. The dots are the experimental data and the lines fits to Eq. (1) with polarization control by quarter-wave plate. (a)–(d) Film-side incidence. (e)–(h) Substrate-side incidence. (a) and (e) Transmitted  $s$  polarized. (b) and (f) Reflected  $s$  polarized. (c) and (g) Transmitted  $p$  polarized. (d) and (h) Reflected  $p$  polarized.

(20) of equations, it is potentially very susceptible to errors. In addition to the statistical errors of coefficients  $f$ ,  $g$ , and  $h$ , we have tested our procedure for its sensitivity to other possible sources of additional inaccuracy (possible vanishing of  $s$ -polarized  $g$  coefficients and possible wave plate retardation errors) in the values of these coefficients. The results of the error analysis are also summarized in Table I. The uncertainties represent the worst-case situation in which the real and imaginary parts of each tensor component are separately pushed to their extrema. The accuracy of most tensor components is satisfactory; however, the error is seen to accumulate in certain components. As encountered in procedures for determining the tensor components of achiral surfaces,  $\chi_{zzz}^{eee}$  has the largest uncertainty of the electric-dipole-allowed components.<sup>20</sup> In addition, some of the small components of  $\chi^{em}$  and  $\chi^{mee}$  have rather large relative errors. In spite of this, we are confident of the results in general. In particular, during our extensive error analysis, the largest tensor components were always the same. Also, our procedure found no good solutions if any of the components with reasonably stable values (indicated by an asterisk in Table I) was assumed to vanish.

Further confidence in our results is provided by their excellent agreement with expected results. We observed the common result that the electric-dipole components  $\chi_{xxz}^{eee}$  and  $\chi_{zxx}^{eee}$  are approximately equal, whereas  $\chi_{zzz}^{eee}$  is somewhat larger.<sup>20,21</sup> Furthermore, the components of  $\chi^{em}$  are larger than those of  $\chi^{mee}$ , as predicted theoretically.<sup>22</sup>

The largest components of the tensors  $\chi^{em}$  and  $\chi^{mee}$  are chiral. Furthermore, these components are larger than the chiral component of  $\chi^{eee}$ . Hence the strongest magnetic quantities are directly associated with the structural asymme-

try of the material. This result is in agreement with the interpretation that large magnetic effects in chiral materials arise from an effective charge displacement along a helical path. For a racemic (50/50) mixture of the two enantiomers, the chiral components would vanish by symmetry, and the relative importance of magnetic contributions would be reduced. For our material, the magnitude of the largest magnetic tensor component is  $\sim 20\%$  of that of the largest electric component. In our error analysis, we have separately considered this ratio, and found it to exceed 16%. The value of  $\sim 20\%$  is in no contradiction with the possible strengths of magnetic-dipole transitions of chiral materials,<sup>4</sup> however, it is significantly larger than estimated earlier.<sup>7,14</sup> This large value could also be due to near-random distribution of the nonlinear chromophores in the polymer film,<sup>23</sup> which tends to suppress the electric-dipole nonlinearity.

We have also considered other possible explanations to our results. Linear optical activity in light propagation through the finite thickness ( $\sim 35$  nm) of our film could mix the  $p$ - and  $s$ -polarized signals and lead to errors. However, we estimate that the maximum linear rotation in our film is a negligible  $0.002^\circ$ . We also note that electric-quadrupole effects, which can be artificially strong due to the large electric-field gradient at a surface,<sup>24</sup> cannot be ruled out by symmetry. Such a surface gradient contribution is localized to a very thin transition layer between two media, whereas the ordinary (“bulk of the film”) quadrupole contribution builds up through the whole thickness of the film. Hence the relative importance of the surface gradient contribution increases as the thickness of the film is decreased. The presence of significant quadrupole contributions is then expected to lead to changes in the measured second-harmonic line

TABLE II. Tensor components determined within electric-dipole approximation and normalized to  $\chi_{xxz}^{eee} = 1$ . The four independent solutions were obtained by considering each measured signal separately (Ref. 15).

Component	Film incidence, transmitted	Film incidence, reflected	Glass incidence, transmitted	Glass incidence, reflected
$zzz$	$-0.483 + i1.143$	$1.610 - i0.381$	$-1.603 + i0.437$	$0.996 - i0.090$
$xxz$	1.00	1.00	1.00	1.00
$zxx$	$0.991 - i0.050$	$0.918 - i0.038$	$0.812 + i0.073$	$1.174 - i0.331$
$xyz$	$0.109 + i0.060$	$0.129 + i0.038$	$0.106 + i0.061$	$0.090 + i0.084$

shapes as the thickness of the film is varied. To address this question, we have also studied a six-layer sample for which the surface gradient contribution is estimated to be  $\sim 12$  times higher than the ordinary quadrupole contribution. No changes in the line shapes indicative of quadrupole effects were observed. Also, our equations cannot be properly solved within the assumption of a surface gradient nonlinearity. These results strongly suggest that quadrupole contributions, if present, are relatively unimportant. Hence the magnetic contributions, whose significance in chiral media is well established, provide the most natural explanation to our results. Finally, we note that our technique could also be applied to the separation of electric-quadrupole and electric-dipole effects.

In conclusion, we determined the relative values of the components of the tensors  $\chi^{eee}$ ,  $\chi^{eem}$ , and  $\chi^{mee}$  that describe second-harmonic generation from a thin film of a chiral polymer. Our experimental technique uses a quarter waveplate to continuously vary the state of polarization of the fundamental beam, and records the intensities of several second-

harmonic signals. No mutual calibration of different signals nor mixing of  $p$ - and  $s$ -polarized signals is necessary. Hence the technique is limited only by the accuracy of individual measurements. This makes it possible to determine the relative values of a very large number (15) of independent tensor components. In this initial demonstration of the technique, a satisfactory accuracy was achieved. For a chiral poly(isocyanide) film, the magnitude of the largest magnetic tensor component is  $\sim 20\%$  of that of the largest electric-dipole component. The largest magnetic components are associated with the chirality of the material, and these components are larger than the chiral component of the electric-dipole-allowed tensor.

We acknowledge the financial support of the Belgian Government (IUAP-16), the Belgian National Science Foundation (FKFO 9.0103.93), and the University of Leuven (GOA95/1). We are grateful to M. N. Teerenstra, A. J. Schouten, and R. J. M. Nolte for providing us with the poly(isocyanide) sample.

- 
- <sup>1</sup>See for example, *Selected Papers on Natural Optical Activity*, edited by A. Lakhtakie (SPIE, Bellingham, WA, 1990).
- <sup>2</sup>J. A. Giordmaine, *Phys. Rev.* **138**, A1599 (1965); Y. T. Lam and T. Thirunamachandran, *J. Chem. Phys.* **77**, 3810 (1982); G. Wagnière, *ibid.* **77**, 2786 (1982).
- <sup>3</sup>P. M. Rentzepis, J. A. Giordmaine, and K. W. Wecht, *Phys. Rev. Lett.* **16**, 792 (1966); A. P. Shkurinov, A. V. Dubrovskii, and N. I. Koroteev, *ibid.* **70**, 1085 (1993); H. Ashitaka *et al.*, *Nonlinear Opt.* **4**, 281 (1993).
- <sup>4</sup>E. W. Meijer, E. E. Havinga, and G. L. J. A. Rikken, *Phys. Rev. Lett.* **65**, 37 (1990); E. W. Meijer and E. E. Havinga, *Synth. Met.* **55-57**, 4010 (1993).
- <sup>5</sup>T. Petralli-Mallow *et al.*, *J. Phys. Chem.* **97**, 1383 (1993); M. J. Crawford *et al.*, *Chem. Phys. Lett.* **229**, 260 (1994).
- <sup>6</sup>M. Kauranen *et al.*, *Adv. Mater.* **7**, 641 (1995).
- <sup>7</sup>M. Kauranen *et al.*, *J. Chem. Phys.* **101**, 8193 (1994).
- <sup>8</sup>T. Verbiest *et al.*, *J. Chem. Phys.* **103**, 8296 (1995).
- <sup>9</sup>J. D. Byers, H. I. Lee, and J. M. Hicks, *J. Chem. Phys.* **101**, 6233 (1994).
- <sup>10</sup>J. D. Byers *et al.*, *Phys. Rev. B* **49**, 14 643 (1994); J. D. Byers and J. M. Hicks, *Chem. Phys. Lett.* **231**, 216 (1994).
- <sup>11</sup>L. Hecht and L. D. Barron, *Mol. Phys.* **89**, 61 (1996).
- <sup>12</sup>M. Kauranen, T. Verbiest, and A. Persoons, *Nonlinear Opt.* **8**, 243 (1994).
- <sup>13</sup>J. J. Maki, M. Kauranen, and A. Persoons, *Phys. Rev. B* **51**, 1425 (1995).
- <sup>14</sup>M. Kauranen, J. J. Maki, and A. Persoons, *Proc. SPIE* **2527**, 328 (1995).
- <sup>15</sup>J. J. Maki *et al.*, *Phys. Rev. B* (to be published).
- <sup>16</sup>P. S. Pershan, *Phys. Rev.* **130**, 919 (1963).
- <sup>17</sup>O. Roders *et al.*, *Appl. Phys. B* **59**, 537 (1994); F. Geiger *et al.*, *ibid.* **61**, 135 (1995).
- <sup>18</sup>J. E. Sipe, *J. Opt. Soc. Am. B* **4**, 481 (1987).
- <sup>19</sup>M. N. Teerenstra *et al.*, *Thin Solid Films* **248**, 110 (1994).
- <sup>20</sup>B. Dick *et al.*, *Appl. Phys. B* **38**, 107 (1985).
- <sup>21</sup>T. F. Heinz, H. W. K. Tom, and Y. R. Shen, *Phys. Rev. A* **28**, 1883 (1983).
- <sup>22</sup>Z. Shuai and J.-L. Brédas (private communication).
- <sup>23</sup>M. N. Teerenstra, Ph. D. thesis, University of Groningen, Groningen, The Netherlands, 1995.
- <sup>24</sup>S. S. Jha, *Phys. Rev.* **140**, A2020 (1965); N. Bloembergen *et al.*, *ibid.* **174**, 813 (1968); P. Guyot-Sionnest, W. Chen, and Y. R. Shen, *Phys. Rev. B* **33**, 8254 (1986); P. Guyot-Sionnest and Y. R. Shen, *ibid.* **35**, 4420 (1987); **38**, 7985 (1988).